Optimized Intermolecular Potential for Aromatic Hydrocarbons Based on Anisotropic United Atoms. III. Polyaromatic and Naphthenoaromatic Hydrocarbons

M. Göktuğ Ahunbay,*,† Javier Perez-Pellitero,§ R. Oliver Contreras-Camacho,§ Jean-Marie Teuler,† Philippe Ungerer,†,‡ Allan D. Mackie,§ and Véronique Lachet‡

Laboratoire de Chimie Physique, Université de Paris Sud, Bâtiment 349, 91405 Orsay Cedex, France, Institut Français du Pétrole, 1-4 Av. de Bois Préau, 92852 Rueil-Malmaison Cedex, France, and Departament d'Enginyeria Química, ETSEQ, Universitat Rovira i Virgili, Avinguda dels Països Catalans, 26. Campus Sescelades, 43007 Tarragona, Spain

Received: October 5, 2004; In Final Form: November 29, 2004

In this third article of the series, a new anisotropic united atoms (AUA) intermolecular potential parameter set has been proposed for the carbon force centers connecting the aromatic rings of polyaromatic hydrocarbons to predict thermodynamic properties using both the Gibbs ensemble and *NPT* Monte Carlo simulations. The model uses the same parameters as previous AUA models used for the aromatic CH force centers. The optimization procedure is based on the minimization of a dimensionless error criterion incorporating various thermodynamic data of naphthalene at 400 and 550 K. The new model has been evaluated on a series of polyaromatic and naphthenoaromatic hydrocarbons over a wide range of temperatures up to near-critical conditions. Vaporization enthalpy, liquid density, and normal boiling temperature are reproduced with good accuracy. The new potential parameters have also been tested successfully on toluene, 1,3,5-trimethylbenzene, styrene, *m*-xylene, *n*-hexylbenzene, and *n*-dodecylbenzene to demonstrate their transferability to alkylbenzenes.

1. Introduction

The development of realistic and efficient potential models for molecular interactions is a crucial requirement for obtaining accurate thermodynamic predictions via molecular simulation techniques including the Gibbs ensemble method, which allows for the efficient determination of liquid−vapor equilibrium properties by Monte Carlo (MC) simulation.[1] For this purpose, several types of intermolecular potentials have been proposed to provide quantitative predictions for hydrocarbons. The most common type of potential is based on the concept of the united atoms (UA), in which the carbon and its bonded hydrogens are represented by a single Lennard-Jones (LJ) force center, with the interaction site being located at the carbon nucleus. Several UA models have been developed in the past,[2−5] which provide satisfactory results, but the search for more quantitative calculations has motivated the investigation of alternative models such as the exponential-6 potential[6] and all-atom[7] models.

Another alternative potential model is the anisotropic united atoms (AUA) model, that is, united atoms, in which the Lennard-Jones interaction site is offset from the carbon nucleus to be shifted toward the hydrogen atoms.[8,9] This potential has been previously developed for *n*-alkanes,[10] branched alkanes,[11] cyclic alkanes,[12] olefins,[13] benzene,[14] and alkylbenzenes.[15] Although its development has required only a small number of parameters, the AUA potential has been shown to provide predictions over a large range of carbon numbers and temperatures. This versatility may be attributed to the physical sense of its parameters, as the offset of the Lennard-Jones sphere allows for a better account of the hydrogens than in the classical united atoms approach.

In the first article of the present series, we proposed a new parametrization of the aromatic CH (ACH−) group parameters with the AUA model based on the vapor−liquid equilibrium properties of benzene.[14] In the second article, we proposed the AUA parameters of the aromatic C (AC−) group of alkyl-substituted benzenes optimized on the phase properties of *p*-xylene.[15] This last model, which has been tested also on several alkylbenzenes and naphthenoaromatics,[16] yielded very accurate estimations of the liquid density and the heat of vaporization, but the overprediction of the saturated vapor pressure was significant.

The purpose of the present article is to extend the AUA potential to polycyclic aromatic hydrocarbons, without reconsidering the parametrization of the ACH[14] nor the parametrization of the CH_2 and CH_3 groups of alkanes.[10] On the other hand, the deviations in the vapor pressures obtained in our studies[15,16] motivated the reparametrization of the AC force centers. For this purpose, we used naphthalene as a reference to calibrate the parameters of the aromatic carbon that connects the aromatic cycles to each other. The transferability of these new parameters has been then tested on the methylenaromatics and alkylbenzenes that were considered in the previous study.[15]

In this article, we present in section 2 the simulation algorithms along with the intermolecular and intramolecular potential energy models. In section 3, we describe the procedure followed to obtain the parameters of the new aromatic carbon group. Section 4 is devoted to the evaluation of the new AUA potential model on polyaromatic (naphthalene, anthracene, and phenanthrene) and naphthenoaromatic (tetralin and decalin) hydrocarbons and its transferability to alkyl-substituted aromatic (toluene, 1,3,5-trimethylbenzene, styrene, *m*-xylene, *n*-hexylbenzene, and *n*-dodecylbenzene) hydrocarbons. Finally, we summarize our conclusions in section 5.

* Corresponding author.
† Université de Paris Sud.
‡ Institut Français du Pétrole.
§ Universitat Rovira i Virgili.

10.1021/jp045474p CCC: $30.25
Published on Web 01/22/2005

TABLE 1: AUA Intermolecular Potentials of Aromatic Hydrocarbons

	σ (Å)	ϵ/k (K)	δ^a (Å)	ref
CH_2	3.461	86.29	0.384	10
CH_3	3.607	120.15	0.216	
ACH	3.246	89.42	0.407	14
AC	3.246	37.72	0	this work

[a] Offset distance between the carbon center and the interaction site.

TABLE 2: Impact of the Molecular Construction on the Accuracy of the Estimated Saturated Vapor Pressures and Liquid Densities of Tetralin and Indan[a]

	average absolute error (%)			
	P_{sat}		ρ_{liquid}	
	ab initio	standard	ab initio	standard
tetralin	20	18	2.6	0.4
indan	16	45	6.1	1.1

[a] Ab initio coordinates were obtained from the NIST Chemistry Webbook[23] for indan and tetralin.

2. Simulation Method

2.1. Potential Energy and Structural Models. The effective intermolecular dispersion−repulsion interactions between two atoms or united atoms, *i* and *j*, were represented by the Lennard-Jones 6-12 equation, using the Lorentz−Berthelot combining rules to compute cross-coefficients in accordance with the preceding works.[10−16] A schematic representation of the AUA model can be found in the first article of the present series.[14] The AUA potential parameters used in this study are given in Table 1.

The bond lengths between atoms were kept constant, and the intramolecular interactions were computed by a summation of bending energy, torsion energy, and distant neighbor interaction energy. The torsion and bending energy parameters were the same as those in our previous work.[15] The distant neighbor energy between groups separated by more than three bonds was computed with the same AUA potential as that for intermolecular interactions.

The aromatic cycles were considered as rigid with hexagonal symmetry.[17−20] In an alkyl substituent on a ring, the carbon in the α position was considered to lie in the aromatic ring plane, with 120° bond angles.[21,22] Consequently, the bending and torsion potentials considered in alkylbenzenes were those involving at least two saturated carbons.

In the case of naphthenoaromatic hydrocarbons (i.e., indan and tetralin), the degrees of freedom available for the bond lengths and angles of the fused structure did not allow for the imposition of identical values for all of the bond lengths and bending angles of the saturated cycle. To overcome this difficulty, two different approaches were tested: (i) to impose the AUA4 parameters to the carbon atoms whose molecular coordinates were obtained from ab initio calculations,[23] where the bond lengths vary between 1.52 and 1.54 Å in the naphthenic ring and between 1.39 and 1.40 Å in the aromatic ring; (ii) to set the bond lengths to the standard values given in our previous study[16] (1.40 Å for the aromatic ring and 1.535 Å for the rest), while fixing bending angles to 120° in aromatic cycles and their first substituents. These two approaches were tested by calculating the phase properties for indan and tetralin. The results were then compared to the data obtained from the DIPPR database.[24] The deviations with respect to DIPPR data, as shown in Table 2, indicated that the first approach yielded a better estimation of the saturated vapor pressure, but it significantly overestimated the liquid densities. As the result of this comparison, the second approach was adopted for the simulations of the naphthenoaromatic hydrocarbons. Furthermore, this choice was logical, since the AUA potential parameters were initially optimized by using standard bond lengths.

2.2. Statistical Ensembles and Monte Carlo Algorithms. Monte Carlo simulations have been carried out in cubic simulation boxes with periodic boundary conditions using the minimum image convention.[25] Dispersion and repulsion interactions were evaluated with a spherical cutoff radius equal to half of the simulation box length, associated with standard long-range corrections.

2.2.1. Gibbs Ensemble Simulations. The vapor−liquid equilibria of the hydrocarbons above the boiling point were calculated using the Gibbs ensemble Monte Carlo method.[1] The MC moves implemented were translations, rigid body rotations, flips,[11,26] configurational bias regrowth and transfers,[2] and volume changes. For rigid molecules, we also used a two-step statistical bias involving the selection of a suitable location for the center of mass in a first step and the test of several orientations in a second step.[12] The probabilities of the MC moves for rigid molecules were generally set as 0.3 for translations and rotations, 0.395 for transfers, and 0.005 for volume changes. In the case of molecules with flexible alkyl chains, typical probabilities were 0.15 for translations, rigid body rotations, flips, and regrowth, 0.395 for transfers, and 0.005 for volume changes. The simulations were carried out using a total of 150 molecules.

Once we have computed the vapor−liquid coexistence density curves, the critical temperature was obtained by fitting the critical scaling law $\rho_l - \rho_v = \lambda(T_c - T)^{0.325}$. The law of rectilinear diameters, $^1/_2(\rho_l + \rho_v) = \rho_c + \gamma(T - T_c)$, was then used to estimate the critical density.

2.2.2. Equilibrium Properties below the Normal Boiling Point. Gibbs ensemble simulations below the normal boiling temperature are problematic because of the very low acceptance ratio of the transfer moves. To overcome this difficulty, simulations below this temperature have been performed in the *NPT* isothermal−isobaric ensemble to calculate the saturated liquid properties. The molar enthalpy of vaporization is given by the following equation:

$$\Delta H_{vap} = -\langle E_{liq(inter)} \rangle + RT \qquad (1)$$

where $\langle E_{liq(inter)} \rangle$ is the average molar intermolecular potential energy in the simulation. This relationship assumes the negligibility of the molar liquid volume compared to the vapor volume and the ideality of the vapor phase. These assumptions are correct below the normal boiling point because of the low density of the saturated vapor. Since liquid properties do not vary significantly between the true vapor pressure and zero pressure, the pressure of the *NPT* simulations has been set to zero. This approximation was checked by carrying out a simulation of liquid naphthalene (352 K) both at zero pressure and at 1 atm, and the differences in the estimated phase properties were found to be smaller than the statistical uncertainties.

To improve the exploration of the configuration space and to take advantage of parallel computers, the *parallel tempering* technique[27] was used with four to eight processors. The acceptance criterion for the exchange of the configurations between temperatures T_i and T_{i+1} was

$$P_{acc} = \min(1, \exp(\Delta\beta\Delta E)) \qquad (2)$$

where $\Delta E = E_{i+1} - E_i$ is the potential energy difference between the configurations and $\Delta\beta = 1/kT_{i+1} - 1/kT_i$ is the difference of the Boltzmann factors.

The details of the thermodynamic integration and the estimation of statistical uncertainties, which is an important aspect in thermodynamic integration, can be found elsewhere.[15] Note that the statistical uncertainties presented in the tables were estimated by the standard block averaging technique[25] and correspond to the 99% confidence level; that is, they are estimated as 2.5 times the standard deviations.

2.3. Optimization Method of Force Field Parameters. To optimize the AUA parameters for the AC force center bonding two aromatic cycles, the following objective function has been used:[10]

$$F = \sum_{i=1}^{n} \frac{(X_i^{\mathrm{mod}} - X_i^{\mathrm{exp}})^2}{s_i^2} \qquad (3)$$

where X_i^{exp} are reference experimental measurements (either ln(P_{sat}), ΔH_{vap}, or ρ_{liq}), X_i^{mod} are the associated computed properties, and s_i are the estimated statistical uncertainty on X_i^{mod} calculated by the block averaging technique. F is considered to be a function of the parameters y_j to be minimized. The minimization of F with respect to all y_j is made by approximating the function by its first-order Taylor expansion. For this purpose, the partial derivatives $\partial X_i^{\mathrm{mod}}/\partial y_k$ are evaluated by the fluctuation method[13] with the initial set of parameters.

3. Determination of Potential Parameters

To improve the accuracy of our estimations, we decided to reoptimize the AUA parameters for the AC force center while keeping the parameters of the ACH group[14] given in Table 1 unchanged. Since the interaction site for an AC group is placed on the carbon nucleus due to symmetry reasons,[15] there are only the two parameters ϵ and σ of the Lennard-Jones potential to determine. For this purpose, we used the optimization method mentioned in section 2.3.

The reference properties defining the objective function were taken from naphthalene, since this molecule contains two AC force centers. The optimization procedure was carried out on the equilibrium properties at 400 and 550 K, which were simulated in the *NPT* and Gibbs ensembles, respectively. While the liquid density and the molar vaporization enthalpy were introduced in the objective function at both temperatures, the saturation pressure was considered only at 550 K. The starting point for the optimization was set as the previously optimized AUA parameters for the AC force center[15] ($\sigma = 3.065$ Å and $\epsilon/k = 42.08$ K). The optimization results showed that the optimum was poorly determined with both variables. This can be explained by the small influence of the AC force center considered on the thermodynamic properties. Consequently, we decided to reduce the number of variables by imposing the LJ diameter to be the same value as for the benzenic CH group. This has the advantage of ensuring a planar geometry of the polyaromatic hydrocarbons. With these constraints, the optimization procedure yielded 37.73 for ϵ/k and 3.246 for σ. A comparison of simulated and reference properties is provided in Table 3.

4. Evaluation of the Optimized AUA Model

The thermodynamic properties of naphthalene calculated with the new parameter set were compared to the experimental data and to the results with the old AUA parameters. The experimental data were obtained from the pseudo-experimental correlations available in the DIPPR database. The result of this comparison shows that the prediction of the saturation pressure is significantly improved, while the predictions of the vaporization enthalpy and the liquid density are still accurate.

The new AUA potential for the AC force center was then tested on several polyaromatics (anthracene, phenanthrene, 1-methylnaphthalene, and 2-methylnaphthalene) and naphthenoaromatics (decalin and tetralin). This evaluation was completed by the calculation of naphthalene properties at other temperatures than those used in the optimization.

The results of the simulations in the Gibbs and *NPT* ensembles for the polyaromatic hydrocarbons are presented in Table 4 and in Figures 1−3, in comparison with the DIPPR data.

The comparison of the predicted values of the liquid density, vaporization enthalpy, and saturated vapor pressures of naphthalene with the DIPPR data indicates that the liquid density and the heat of vaporization are well reproduced. As for the

TABLE 3: Reference Data and Simulation Conditions Used for the Optimization of the Parameters of the Aromatic C Group on Naphthalene Phase Properties

T (K)	ensemble	property	simulation	DIPPR	% error
550	Gibbs	P_{sat} (kPa)	3826	3299	15.97
		ΔH_{vap} (kJ/mol)	39.6	38.3	3.48
		ρ_{liquid} (kg/m^3)	811.3	803.4	0.99
400	*NPT*, $P = 0$	ΔH_{vap} (kJ/mol)	50.6	49.7	1.81
		ρ_{liquid} (kg/m^3)	967.1	941.1	2.76

TABLE 4: Equilibrium Properties of Naphthalene, Phenanthrene, and Anthracene Obtained by Simulation with the Proposed AUA Potential, Compared with the DIPPR Correlations of Experimental Measurements[a]

		ρ_{liquid} (kg/m^3)			ΔH_{vap} (kJ/mol)			P_{sat} (kPa)		
T (K)		AUA	exptl	% dev	AUA	exptl	% dev	AUA	exptl	% dev
Naphthalene										
677	G	$641.6_{14.1}$	637.7	0.6	24.2_{8}	23.8	1.4	2625_{260}	1919	36.8
607	G	$743.8_{10.6}$	738.8	0.7	33.8_{6}	32.7	3.2	1097_{126}	798	37.5
550	G	$811.3_{6.5}$	803.4	1.0	39.6_{4}	38.3	3.5	383_{32}	330	16.0
503	G	$859.9_{6.9}$	850.5	1.1	43.1_{5}	42.2	2.0	155_{10}	133	16.5
463	G	$902.4_{5.3}$	887.1	1.7	46.0_{4}	45.3	1.6	$51.8_{7.2}$	52.0	−0.5
429	N	$937.7_{4.3}$	916.7	2.3	48.7_{3}	47.7	2.1	$23.5_{2.4}$	19.8	18.8
400	N	$967.1_{4.4}$	941.1	2.8	50.6_{3}	49.7	1.8	$7.0_{1.2}$	7.3	−3.9
374	N	$990.6_{4.8}$	961.7	3.0	52.1_{3}	51.4	1.5	2.95_{30}	2.6	11.7
352	N	$1007.7_{2.7}$	979.4	2.9	53.4_{2}	52.8	1.2	0.83_{12}	0.9	−11.2
average absolute deviations:				1.8			2.0			15.5
Phenanthrene										
751	G	$759.4_{10.7}$	744.2	2.0	$43.1_{1.0}$	43.0	0.1	965_{97}	825	16.9
675	G	$854.5_{5.7}$	831.1	2.8	52.5_{6}	50.8	3.4	306_{25}	301	1.6
613	G	$928.5_{3.2}$	889.4	4.4	59.2_{4}	55.7	6.2	134_{10}	107	24.8
561	N	$968.6_{4.4}$	932.6	3.9	63.8_{5}	59.2	7.8	$36.3_{4.5}$	36.8	−1.6
518	N	$1006.6_{5.5}$	966.4	4.2	66.8_{5}	61.8	8.1	$13.4_{1.7}$	12.2	9.8
480	N	$1039.7_{5.7}$	993.8	4.6	69.5_{5}	63.9	8.7	3.25_{41}	3.90	−16.5
448	N	$1060.8_{3.9}$	1016.5	4.4	71.2_{4}	65.6	8.5	1.09_{10}	1.20	−9.5
420	N	$1080.7_{5.0}$	1035.7	4.3	72.9_{6}	67.1	8.7	0.25_{03}	0.36	−31.2
395	N	$1095.2_{3.9}$	1052.1	4.1	74.1_{6}	68.3	8.5	0.08_{01}	0.11	−25.9
average absolute deviations:				4.1			7.6			13.4
Anthracene										
751	G	$735.3_{5.1}$	716.1.	2.7	41.3_{5}	44.5	−7.2	1091_{86}	766	42.4
675	G	$826.0_{6.1}$	805.2	2.6	51.0_{5}	51.1	−0.2	340_{47}	276	23.0
613	G	$893.5_{5.7}$	866.5	3.1	56.9_{5}	55.2	3.1	112_{20}	98.7	13.1
561	N	$949.8_{5.2}$	912.7	4.1	62.4_{5}	58.1	7.4	$43.6_{6.0}$	34.3	27.1
518	N	$988.2_{4.0}$	949.2	4.1	65.6_{4}	60.3	8.8	$11.7_{2.1}$	11.6	1.4
average absolute deviations:				3.3			5.3			16.1[b]

[a] "G" and "N" indicate a simulation in the Gibbs or *NPT* ensemble, respectively. The uncertainties are shown as subscripts. The same representation applies to the rest of the tables. [b] The 751 K point has been excluded.

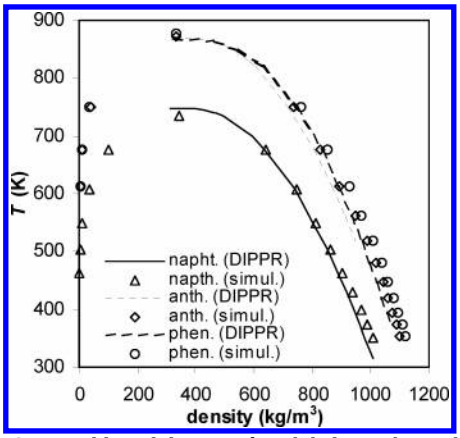

Figure 1. Saturated liquid density of naphthalene, phenanthrene, and anthracene, computed with the new AUA potential. Comparison is given with the correlations of experimental data provided by the DIPPR database.

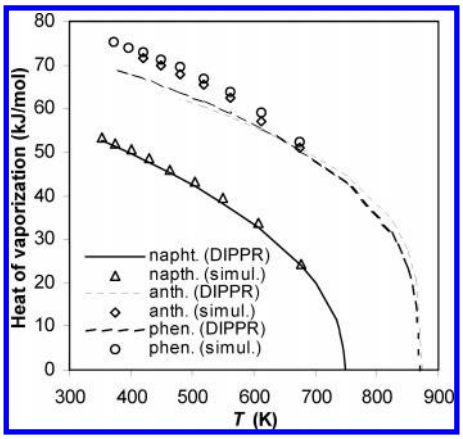

Figure 2. Vaporization enthalpy of naphthalene, phenanthrene, and anthracene, computed with the new AUA potential. Comparison is given with the correlations of experimental data provided by the DIPPR database.

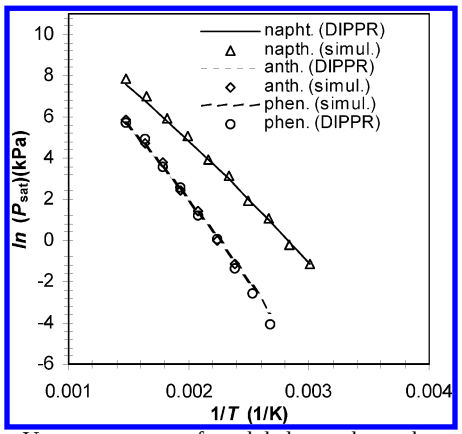

Figure 3. Vapor pressures of naphthalene, phenanthrene, and anthracene, computed with the new AUA potential. Comparison is given with the correlations of experimental data provided by the DIPPR database.

saturated vapor pressure, the deviations from the experimental data decrease with decreasing temperature; consequently, simulations yield 486 K for the normal boiling temperature compared to the experimental value of 490 K.

The tricyclic aromatic molecules, anthracene and phenanthrene, exhibit coherent behaviors with respect to each other with an overestimation of the liquid density and the heat of vaporization. The increase in the overestimation in the liquid density with decreasing temperature is similar to the trend

TABLE 5: Equilibrium Properties of 1-Methylnaphthalene and 2-Methylnaphthalene Obtained by Simulation with the Proposed AUA Potential, Compared with the DIPPR Correlations of Experimental Measurements

		ρ_{liquid} (kg/m^3)			ΔH_{vap} (kJ/mol)			P_{sat} (kPa)		
T (K)		AUA	exptl	% dev	AUA	exptl	% dev	AUA	exptl	% dev
					1-Methylnaphthalene					
647	G	$699.9_{10.0}$	695.7	−0.6	34.4_6	36.3	−5.2	1065_{89}	925	15.1
573	G	$785.1_{3.9}$	803.0	2.3	42.5_4	42.7	−0.5	402_{42}	301	33.7
514	G	$842.6_{4.7}$	858.9	1.9	47.2_4	46.8	0.9	101_{10}	94	7.8
466	N	$885.3_{3.8}$	907.9	2.6	51.5_3	49.6	3.7	$41.5_{4.3}$	28.1	47.6
426	N	$918.5_{2.8}$	945.5	2.9	54.1_3	51.8	4.4	8.5_9	8.1	4.4
393	N	$945.4_{4.5}$	979.6	3.6	56.8_4	53.5	6.1	3.1_3	2.3	35.1
364	N	$967.5_{2.9}$	1008.7	4.3	59.1_3	54.9	7.7	0.55_{06}	0.62	−10.5
				2.6			4.1			22.0
					2-Methylnaphthalene					
647	G	$689.6_{9.5}$	681.5	1.2	32.7_6	34.3	−4.7	1217_{110}	881	38.2
573	G	$777.1_{3.9}$	768.7	1.1	41.3_3	41.5	−0.6	393_{46}	301	30.3
514	G	$849.3_{5.5}$	826.9	2.7	46.8_4	46	1.6	126_9	99.9	26.3
466	N	$891.2_{2.8}$	869.7	2.5	50.6_2	49.2	2.7	$41.3_{6.7}$	31.2	32.5
426	N	$929.1_{4.0}$	903.0	2.9	53.3_3	51.7	3.2	$11.1_{1.0}$	9.1	21
393	N	$958.5_{2.3}$	929.8	3.1	55.5_2	53.6	3.5	3.2_5	2.5	25.8
364	N	$981.3_{3.0}$	951.9	3.1	57.1_2	55.1	3.6	0.77_{06}	0.66	15.8
average absolute deviations				2.4			2.9			27.2

TABLE 6: Equilibrium Properties of Tetralin and Indan Obtained by Simulation with the Proposed AUA Potential, Compared with the DIPPR Correlations of Experimental Measurements

		ρ_{liquid} (kg/m^3)			ΔH_{vap} (kJ/mol)			P_{sat} (kPa)		
T (K)		AUA	exptl	% dev	AUA	exptl	% dev	AUA	exptl	% dev
					Tetralin					
610	G	$678.5_{4.6}$	679.7	−0.2	31.3_3	30.3	3.1	1241_{98}	1001	24.0
575	G	$717.6_{4.6}$	723.0	−0.7	35.2_3	34.2	2.9	656_{62}	602	9.1
543	G	$751.6_{5.2}$	758.1	−0.9	38.1_3	37.2	2.4	365_{39}	357	2.5
490	G	$810.8_{7.4}$	810.9	0.0	42.2_5	41.7	1.4	134_{12}	125	7.7
446	N	$853.1_{4.1}$	850.2	0.3	45.7_2	44.9	1.7	$47.9_{7.2}$	42.2	13.4
410	N	$885.3_{2.7}$	881.1	0.5	47.7_2	47.4	0.7	$14.9_{1.6}$	13.7	8.8
379	N	$912.9_{2.4}$	906.1	0.8	49.6_2	49.4	0.4	4.8_7	4.3	12.5
352	N	$935.1_{3.4}$	926.8	0.9	51.1_3	51.0	0.2	1.4_1	1.3	6.9
average absolute deviations:				0.5			1.6			10.6
					Indan					
590	G	$648.7_{6.8}$	648.2	0.1	26.4_4	27.0	2.3	1623_{123}	1262.2	28.6
550	G	$709.7_{4.9}$	704.8	0.7	31.1_4	31.3	0.8	895_{73}	702.2	27.5
496	G	$777.7_{3.8}$	770.4	0.9	36.2_2	36.1	0.1	326_{42}	270.4	20.6
451	G	$826.5_{3.6}$	818.5	1.0	39.4_2	39.5	0.4	123_{23}	101.3	21.9
414	N	$864.2_{3.0}$	855.7	1.0	42.2_2	42.1	0.2	$49.1_{7.9}$	36.8	33.5
382	N	$895.2_{3.6}$	885.6	1.1	44.0_3	44.1	0.2	$16.2_{3.3}$	12.9	25.8
355	N	$921.1_{2.7}$	910.4	1.2	45.6_2	45.7	0.3	5.9_9	4.4	35.0
331	N	$942.5_{2.8}$	931.2	1.2	46.9_2	47.1	0.4	1.8_3	1.4	25.9
average absolute deviations:				0.9			0.6			27.3

observed with naphthalene. Furthermore, the magnitude of absolute deviations in the vapor pressures is also consistent with that of naphthalene. The boiling temperatures for anthracene and phenanthrene were estimated as 605 and 606 K, respectively, compared to the experimental value 609 K, which is identical for both compounds.

While evaluating the accuracy of these estimates, the errors in the DIPPR correlations must also be taken into consideration. The maximum errors in these correlations, as reported in the DIPPR database, are listed in Table 9. As an example to illustrate the extent of the uncertainties in the correlations, Rojas and Orozco[28] reported the experimental value of the heat of vaporization for anthracene as 66.68 kJ/mol at 498.15 K, which agrees perfectly with our predictions, while the DIPPR correlation at the same temperature yields 61.22 kJ/mol.

The phase properties of 1-methylnaphthalene and 2-methylnaphthalene are presented in Table 5 and Figures 4−6. From the figures, it can be seen that our AUA model well reproduced the differences in the phase properties of these two isomers. The estimated normal boiling temperatures of 1-methylnaphthalene and 2-methylnaphthalene were 506 and 503 K, respectively, compared to the experimental values 517 and 514 K.

TABLE 7: Comparison of Average Absolute Errors in the Predicted Phase Properties of Alkylbenzenes Calculated with the Old (Model I) and New (Model II) Parameters for the Aromatic C Force Center

	average absolute error (%)					
	model I			model II		
	ρ_{liquid}	ΔH_{vap}	P_{sat}	ρ_{liquid}	ΔH_{vap}	P_{sat}
1,3,5-trimethylbenzene	1.0	7.6	43.0	1.1	1.8	24.4
toluene	1.3	4.7	24.9	0.4	1.0	12.2
styrene	0.1	0.9	18.0	0.5	1.0	29.0
m-xylene	1.2	4.2	34.7	1.8	1.5	33.2
n-hexylbenzene	1.2	2.0	15.3	1.3	2.6	15.6
n-dodecylbenzene	1.6	1.7	38.4	1.4	1.8	29.8
overall absolute error	1.1	3.5	29.0	1.1	1.6	24.0

TABLE 8: Estimated Critical Temperature, Critical Density, and Normal Boiling Temperature of the Polyaromatics and Naphthenoaromatics Considered[a]

	T_c (K)			ρ_c (kg·m^{-3})			T_b (K)		
	AUA	exptl	% dev	AUA	exptl	% dev	AUA	exptl	% dev
naphthalene	734	748	−1.9	331	315	5.0	486	490	−0.9
1-methylnaphthalene	757	772	−2.0	312	307	1.5	506	517	−2.0
2-methylnapahtalene	759	761	−0.3	322	305	5.5	503	514	−2.2
anthracene	873	873	0.0	333	322	3.5	605	609	−0.7
phenanthrene	876	869	0.8	333	322	3.5	606	609	−0.5
tetralin	723	721	0.3	312	322	−3.2	477	481	−0.8
indan	684	685	−0.1	307	298	2.8	442	451	−2.1
average absolute deviation (%)			0.8			3.6			1.3

[a] The computed values (AUA) are compared with the DIPPR data.

TABLE 9: Comparison of Average Absolute Errors in the Predicted Phase Properties of Polyaromatics and Naphthenoaromatics Calculated with the Old (Model I) and New (Model II) Parameter Set for the Aromatic C Force Center[a]

	average absolute error (%)								
	model I			model II			max DIPPR error (%)		
	ρ_{liquid}	ΔH_{vap}	P_{sat}	ρ_{liquid}	ΔH_{vap}	P_{sat}	ρ_{liq}	ΔH_{vap}	P_{sat}
naphthalene	2.6	2.3	28.7	1.8	2.0	15.5	3	3	1
anthracene	3.8	5.4	65.2	3.5	4.8	16.1	5	3	3
phenanthrene	4.5	6.2	30.3	4.1	7.6	13.4	3	3	3
tetralin	0.5	0.6	15.7	0.5	1.6	10.6	3	5	3
indan	1.1	1.7	44.6	0.9	0.6	27.3	5	5	3
overall absolute error	2.3	3.5	34.9	1.9	2.9	15.9			

[a] The table includes also maximum errors reported in the DIPPR correlations.

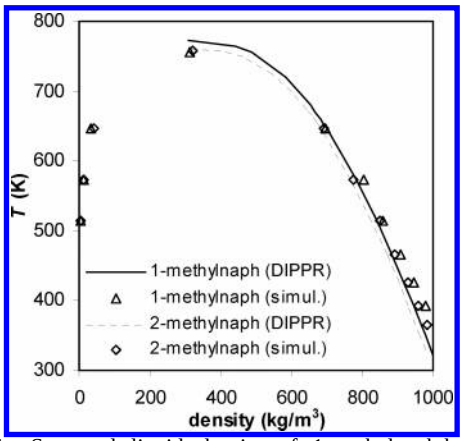

Figure 4. Saturated liquid density of 1-methylnaphthalene and 2-methylnaphthalene, computed with the new AUA potential. Comparison is given with the correlations of experimental data provided by the DIPPR database.

Finally, the result of simulations in the Gibbs and *NPT* ensembles for the naphthenoaromatic hydrocarbons are presented in Table 6 and in Figures 7−9. The comparison of the predicted properties with the DIPPR data for tetralin and indan shows that these properties are overall very well reproduced. The normal boiling point of tetralin was estimated as 477 K with respect to 481 K, the experimental value. As for indan, the underestimation in the normal boiling point (442 K) is slightly larger compared to the experimental value (451 K).

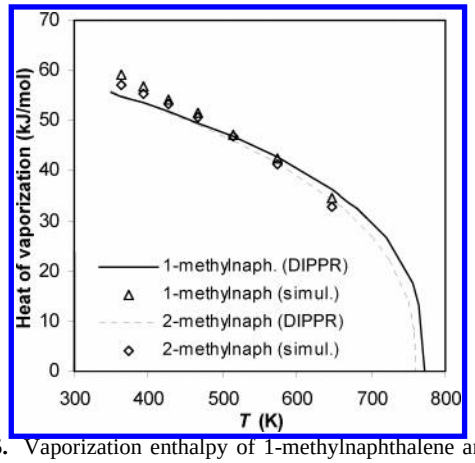

Figure 5. Vaporization enthalpy of 1-methylnaphthalene and 2-methylnaphthalene, computed with the new AUA potential. Comparison is given with the correlations of experimental data provided by the DIPPR database.

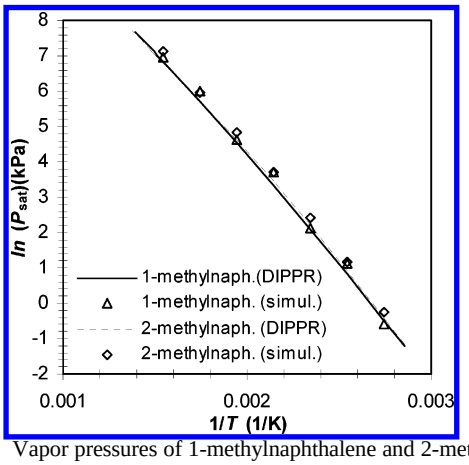

Figure 6. Vapor pressures of 1-methylnaphthalene and 2-methylnaphthalene, computed with the new AUA potential. Comparison is given with the correlations of experimental data provided by the DIPPR database.

The transferability of this new set of parameters was also tested on toluene, 1,3,5-trimethylbenzene, styrene, *m*-xylene, *n*-hexylbenzene, and *n*-dodecylbenzene. The result of these comparisons is presented in Table 7 and indicates that the previously optimized parameters[15] for the AC force centers can be replaced with the new ones.

The critical temperature and the critical density of the hydrocarbons investigated are given in Table 8 along with the normal boiling temperature. The comparison of the estimated values with experimental data shows very good agreement, especially for the critical densities and the boiling points.

Overall evaluation of the results shows that the accuracy in the estimations of the thermodynamic properties has improved with the new AUA parameters for the AC group, as can be seen in Table 9. The table provides a comparison of accuracies in the estimated phase properties calculated with the old and new parameters for the AC group. This improvement is especially significant for the saturated vapor pressures, which is reflected in the accurate prediction of the normal boiling points with an average error of 1.3%.

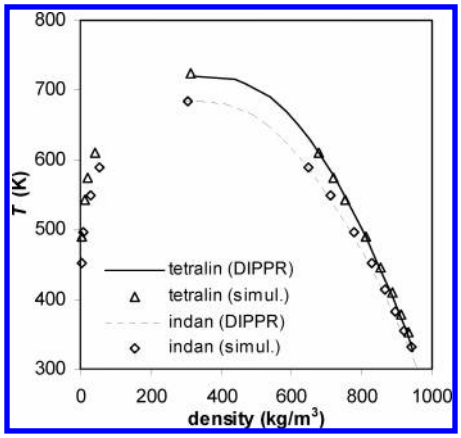

Figure 7. Vapor and liquid densities of tetralin and indan. Simulation results obtained with the new AUA potential are compared with the correlations of the DIPPR database.

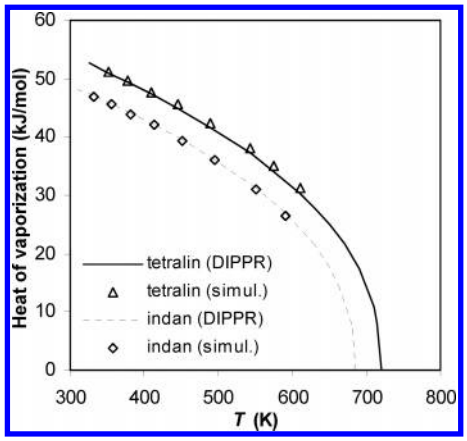

Figure 8. Vaporization enthalpy of tetralin and indan. Simulation results obtained with the new AUA potential are compared with the correlations of the DIPPR database.

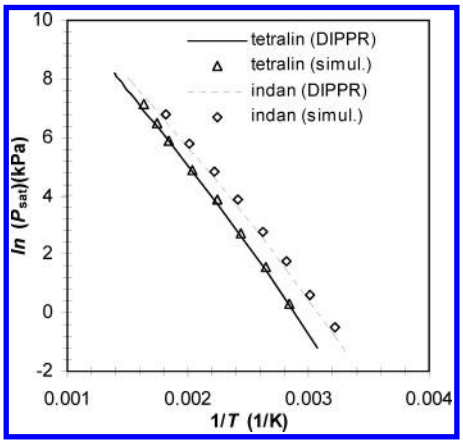

Figure 9. Saturated vapor pressure of tetralin and indan. Simulation results obtained with the new AUA potential are compared with the correlations of the DIPPR database.

5. Conclusion

In this work, we propose an AUA parameter set for the C force centers for polyaromatic hydrocarbons based on an optimization of the phase properties of naphthalene. The Lennard-Jones diameter of this AC force center has been imposed to be identical to the ACH force center, which is more consistent because it confers a planar geometry to the polyaromatic units. This new parameter set (Table 1) provides good predictions for polycyclic aromatics and naphthenoaromatics in the present study, with heats of vaporization, liquid densities, and normal boiling temperatures predicted with satisfactory accuracy. The average absolute errors in these properties were 2.9, 1.9, and 1.3%, respectively.

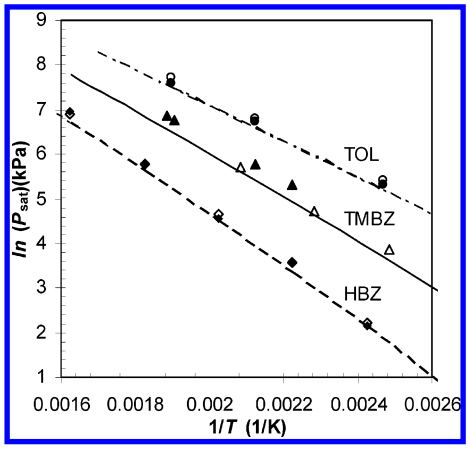

Figure 10. Comparison of the saturated vapor pressure for toluene (TOL), 1,3,5-trimethylbenzene (TMBZ), and *n*-hexylbenzene (HBZ) estimated with model I[15] (solid symbols) and model II (this work; open symbols) for AC force centers. The lines represent the DIPPR data. Note the overlapping symbols for *n*-hexylbenzene due to scaling.

The transferability of the new parameter set for the aromatic carbon was also tested on toluene, 1,3,5-trimethylbenzene, styrene, *m*-xylene, *n*-hexylbenzene, and *n*-dodecylbenzene. The results for the vapor pressure are presented in Figure 10, in comparison with those obtained previously with the AC force center calibrated on *p*-xylene. The vapor pressures of toluene and trimethylbenzene appear better predicted with the parameters of the AC group. A similar improvement is also found for the vaporization enthalpy of these two molecules. In the case of *n*-hexylbenzene, the new parameters for the AC group provide equivalent predictions of the vapor pressure and the vaporization enthalpy. Finally, for *n*-dodecylbenzene, a significant improvement can be observed in the estimation of its vapor pressure. As summarized in Table 7, the average error drops from 3.5 to 1.6% for the vaporization enthalpy and from 29.0 to 24.0% for the saturation pressure and remains at 1.1% for the saturated liquid density.

Acknowledgment. M.G.A. thanks the company Total for financial support, and the authors personally thank François Montel for his interest in the work and fruitful discussions. R.O.C.-C., J.P.-P., and A.D.M. acknowledge financial support from the *Ministerio de Ciencia y Tecnología* of the Spanish Government (CTQ2004-03346/PPQ and MAT2002-11990-E), the *Generalitat de Catalunya* (ACI 2003-22) , as well as the Universitat Rovira i Virgili.

References and Notes

(1) Panagiotopoulos, A. Z. *Mol. Phys.* **1987**, *61*, 813.
(2) Smit, B.; Karaborni, S.; Siepmann, I. J. *J. Chem. Phys.* **1995**, *102*, 2126.
(3) Martin, M. G.; Siepmann, J. I. *J. Phys. Chem. B* **1998**, *102*, 2569.
(4) Nath, S. A.; Escobedo, F. A.; de Pablo, J. J. *J. Chem. Phys.* **1998**, *108*, 9905.
(5) Lopez-Rodriguez, A.; Vega, C.; Freire, J. J. *J. Chem. Phys* **1999**, *111*, 438.
(6) Errington, J. R.; Panagiotopoulos, A. Z. *J. Phys. Chem. B* **1999**, *103*, 6314.
(7) Chen, B.; Siepmann, I. J. *J. Phys. Chem.* **1999**, *103*, 5370−5379.
(8) Toxvaerd, S. *J. Chem. Phys.* **1990**, *93*, 4290.
(9) Toxvaerd, S. *J. Chem. Phys.* **1997**, *107*, 5197.
(10) Ungerer, P.; Beauvais, C.; Delhommelle, J.; Boutin, A.; Rousseau, B.; Fuchs, A. H. *J. Chem. Phys.* **2000**, *112*, 5499.

(11) Bourasseau, E.; Ungerer, P.; Boutin, A.; Fuchs, A. H. *Mol. Simul.* **2002**, *28*, 317.
(12) Bourasseau, E.; Ungerer, P.; Boutin, A. *J. Phys. Chem. B* **2002**, *106*, 5483.
(13) Bourasseau, E.; Haboudou, M.; Boutin, A.; Fuchs, A. H.; Ungerer, P. *J. Chem. Phys.* **2003**, *118*, 3020.
(14) Contreras-Camacho, O.; Ungerer, P.; Boutin, A.; Fuchs, A. H.; Mackie, A. D. *J. Phys. Chem. B* **2004**, *108*, 14109.
(15) Contreras-Camacho, O.; Lachet, V.; Ahunbay, M. G.; Perez, J.; Ungerer, P.; Boutin, A.; Mackie, A. D. *J. Phys. Chem. B* **2004**, *108*, 14115.
(16) Ahunbay, M. G.; Kranias, S.; Lachet, V.; Ungerer, P. *Fluid Phase Equilib.* **2004**, *224*, 73.
(17) Errington, J. R.; Panagiotopoulos, A. Z. *J. Chem. Phys.* **1999**, *111*, 9731.
(18) Friedrich, A.; Lustig, R. *J. Mol. Liq.* **2002**, *98*, 241.
(19) Evans, D. J.; Watts, R. O. *Mol. Phys.* **1976**, *32*, 93.
(20) Jorgensen, W. L.; Severance, D. L. *J. Am. Chem. Soc.* **1990**, *112*, 4768.
(21) Jorgensen, W. L.; Laird, E. R.; Nguyen, T. B.; Tirado-Rives, J. *J. Comput. Chem.* **1993**, *14*, 206.
(22) Wick, C. D.; Martin, M. G.; Siepmann, J. I. *J. Phys. Chem B* **2000**, *104*, 8008.
(23) Linstrom, P. J.; Mallard, W. G., Eds. *NIST Chemistry WebBook, NIST Standard Reference Database Number 69* (http://webbook.nist.gov); National Institute of Standards and Technology: Gaithersburg, MD, 2003.
(24) Rowley, R. L.; Wilding, W. V.; Oscarson, J. L.; Zundel, N. A.; Marshall, T. L.; Daubert, T. E.; Danner, R. P. *DIPPR Data Compilation of Pure Compound Properties*; Design Institute for Physical Properties, AIChE: New York, 2002.
(25) Allen, M. P.; Tildesley, D. J. *Computer simulation of liquids*; Oxford Science Publications: Oxford, U.K., 1987.
(26) Dodd, L. R.; Boone, T. D.; Theodorou, D. N. *Mol. Phys.* **1993**, *78*, 961.
(27) Yan, Q.; de Pablo, J. J. *J. Chem. Phys.* **1999**, *111*, 9509.
(28) Rojas, A.; Orozco, E. *Thermochim. Acta* **2003**, *405*, 93−107.